

Climate Change in Canadian Floodplain Mapping Assessments

Final Report developed under Contract #3000704047 for
Natural Resources Canada

Centre for Hydrology Report No. 17

Chandra Rajulapati, Zelalem Tesemma, Kevin Shook, Simon Papalexiou, and
John W Pomeroy

Centre for Hydrology, University of Saskatchewan
101-121 Research Drive, Saskatoon, Saskatchewan S7N 1K2



Climate Change in Canadian Floodplain Mapping Assessments

Centre for Hydrology Report No. 17

Chandra Rajulapati, Zelalem Tesemma, Kevin Shook, Simon Papalexiou, and
John W Pomeroy

Centre for Hydrology, University of Saskatchewan
101-121 Research Drive, Saskatoon, Saskatchewan S7N 1K2

April 30, 2020

Prepared for Natural Resources Canada

© 2020 Centre for Hydrology, University Saskatchewan, Saskatoon, Saskatchewan

Contact:

Professor John W Pomeroy, PhD, FRSC, FRGS
Director, Centre for Hydrology
University of Saskatchewan
101 – 121 Research Drive,
Saskatoon, Saskatchewan, Canada
S7N 1K2

john.pomeroy@usask.ca
www.usask.ca/hydrology

Context and Executive summary

In the recent decades, precipitation patterns and corresponding streamflow responses in many cold regions catchments have changed considerably due to warming. Understanding historical changes and predicting future responses are of great importance for planning and management of water resources systems. Regional climate simulations using convention-permitting models are helpful in representing the fine-scale cloud and mesoscale processes, which are critical for understanding the physical mechanisms that cause in convective precipitation. From a hydrological perspective, these fine resolution simulations are helpful in understanding the runoff generation mechanisms, particularly for mountainous watersheds, which have high spatial variation in precipitation due to large differences in elevation over small distances.

Natural Resources Canada (NRCan) is developing the Federal Flood Mapping Guidelines Series to support the National Disaster Mitigation Program (NDMP) led by Public Safety Canada (PS). These documents are developed through consultation with practitioners and stakeholders including the Federal Flood Mapping Committee (FMC) chaired by NRCan and PS, and the 175 members of the Technical Working Group (TWG). The TWG comprises technical experts and practitioners from across Canada, and includes several sub-groups including the Climate Change Sub-Group. The Guideline Series is intended to move toward common practices in flood mapping across Canada and are published for all Canadians. NRCan published the “Case Studies on Climate Change and Floodplain Mapping” in 2018, which offered insight into incorporating climate change projections into flood mapping studies at three locations in Canada. This was followed by a publication by the National Research Council (NRC) in March 2019 titled “An Inventory of Methods for Estimating Climate Change-Informed Design Water Levels for Floodplain Mapping”, which describes current practices across Canada for incorporating climate change into flood mapping studies.

Global Water Futures (GWF) conducted a study on “Historical and Future Flow Regimes at the Bow River in Calgary” referred to as the Bow River Basin Study (BRBS) with funding support from NRCan’s Climate Change Impacts Adaptation Division (CCIAD). This project offered insight into the effects of climate change on flow in that watershed. GWF indicated that the ‘next steps’ for that work were to: prepare a case study report on how climate change may affect future flood flows that could be applied to floodplain mapping; and, detail how climate change can be downscaled and applied in large scale hydrological assessments of impacts on hydrological regimes.

The sister-study of this report, the Bow River Basin Study (BRBS), used a physically based hydrological land surface scheme along with a water management model, coupled with a high resolution convention-permitting atmospheric regional model (Weather Research and Forecasting, WRF) to understand the streamflow generating mechanisms and identify the changes in streamflow responses of the Bow and Elbow River Basins. The coupled model appears to provide a large improvement in predictability, with minimal calibration of parameters and without bias correction of forcing from the atmospheric model. The model

was able to provide reliable estimates of streamflows, despite the complex topography in the catchment. Using the WRF Pseudo Global Warming (PGW) scenario, estimated future streamflows simulated were then used to develop projected flow exceedance curves. The uncertainty in the simulations is extremely helpful in the risk assessment for downstream flood inundations. However, the uncertainty in streamflows cannot be assessed as the WRF-PGW dataset was only available for a single realization, because of the high computational cost.

The research presented in this report focusses instead on using the highly efficient hydrological model developed and verified in BRBS whilst assessing uncertainty using another regional climate model, the CanRCM4, where many realizations are available for different boundary conditions. Since the CanRCM4 simulations have a relatively low resolution, a novel methodology was developed to adjust regional climate model outputs using the WRF-PGW data. An ensemble of 15 CanRCM4 simulations was used to force the Bow River basin model to determine a measure of the uncertainty in the simulated streamflows, and the projected streamflow exceedance probability curves. These curves are extremely useful for risk assessment for downstream flood inundations. Given the importance of understanding how much extreme precipitation will change in urban areas of the basin, where short duration high intensity events cause flash flooding, frequency analysis of these events was carried out for Calgary and Intensity Duration Frequency (IDF) curves were developed. A ready-to-use empirical form of IDF curve has been proposed from this analysis for the City of Calgary.

The results from the WRF-PGW modelling indicated that future high flow, low frequency (exceedances less than 10%) streamflow events will decrease compared to those under the current climate condition by 4, 9 and 1.6 m³/s for the Bow River at Banff and Calgary and Elbow River at Sarcee Bridge respectively. The average of the 15 new CanRCM4-WRF-PGW results supports the above result with some greater decreases in streamflow of 9, 16 and 4 m³/s for Bow River at Banff and Calgary and Elbow River at Sarcee Bridge respectively. However, there were some CanRCM4-WRF-PGW realisations that suggested substantial increases in future low frequency streamflow from those indicated by the average CanRCM4-WRF-PGW-drive MESH model. The below average, high frequency (exceedances greater than 30%) future streamflows will increase modestly in all gauging locations by from 1 to 12.5 m³/s.

The results of the extreme precipitation analysis at Calgary indicated an increase in future extreme precipitation events of all duration and return periods. On an average an increase of 1.5 times is noted for short return periods (=2, 5), and an increase of 4 times for long return periods (=500, 1000).

Finally, this study provides a blueprint for other studies that aims in assessing the impact of future climate change on the streamflow and flood frequency analysis for major rivers that flow into urban areas and it can be taken as a pilot study for Canada. The study highlights the usefulness of multi-CanRCM4 realisations and high-resolution WRF model outputs in studies of the hydrological impacts of climate change. The flow duration curves developed from this study can be used to estimate flood frequency for floodplain mapping purposes if they are

used as inputs to locally developed hydraulic models of the region of interest. The methodology shown here can be applied to river basins flowing into communities of interest across Canada. As a precondition for such applications a national gridded database of high resolution (4 km) WRF model downscaled climate model outputs that have been perturbed by multiple bias-corrected regional climate model realisations should be prepared as a national forcing dataset for hydrological model applications. The MESH hydrological model evaluated here performed quite well when driven by high resolution WRF model outputs and should be examined for national application to force local hydraulic models of flood inundation elsewhere in Canada. This would be the basis for a coherent national approach to floodplain mapping that takes into account both non-stationarity due to climate change and uncertainty from climate models. Adopting this state-of-the-art approach would make Canada a global leader in assessing the risks of changing flooding due to climate change.

Table of Contents

1. Introduction	7
2. Study Area and Data	7
2.1 Study area	7
2.2 Data	8
2.2.1 WRF-ERA40 and WRF-PGW modelling	8
2.2.2 CanRCM4 data	8
3. Methodology	9
3.1 CanRCM4 precipitation frequency distributions to perturb WRF precipitation fields	9
3.2 Frequency analysis of precipitation at Calgary	11
3.3 MESH runs using historical WRF and CanRCM4 perturbed WRF-PGW	13
4. Results	15
4.1 WRF-Historical and WRF-PGW Meteorology	15
4.2 CanRCM4 Meteorology	17
4.3 CanRCM4 perturbed WRF-PGW Meteorology	18
4.4 Change in extreme precipitation at Calgary	21
4.5 MESH driven using historical WRF meteorological forcing	23
4.6 Assessment of change to extreme streamflow events using CanRCM4 uncertainty and WRF-PGW forcing data	24
5. A blueprint for calculating future streamflow discharges and their probabilities for Canada	30
5.1 Assessment of uncertainty	30
5.2 Considerations in applying this pilot project to other basins	30
5.3 How to drive hydraulic models of flood plains using these outputs	30
6. Conclusions	33
7. References	34

1. Introduction

Flood plain mapping and delineation are important for urban evolution and development near river floodplains, as they allow the development of adaptation and mitigation strategies. Flooding in cold regions may result from several hydrometeorological mechanisms such as snowmelt runoff, rainfall, rain-on-snowmelt and river ice jams. In recent decades, warming trends and other changes in climate have driven rapid changes in cold regions, disturbing the water cycle and changing the responses of earth systems (Fang & Pomeroy, 2007; Trenberth, 2011). Understanding historical changes and better predicting future responses are of great importance for adaptation and mitigation.

A MESH (Modélisation Environnementale communautaire - Surface Hydrology) hydrological model was developed for the Bow River Basin Study (BRBS) to quantify the flood generating mechanisms and their changes in the future (Tesemma et al., 2020). The study reported on here builds on the BRBS results and provides estimates of uncertainty using a suite of 15 simulations from the CanRCM4 regional climate model to characterize the uncertainty and variation over time of global climate outcomes. This variability was utilized to perturb 15-year runs of the Weather Research and Forecasting (WRF) model in Pseudo-Global Warming (PGW) mode by substituting new statistical distributions of precipitation for the WRF precipitation fields. These perturbed WRF outputs were then used as forcing for 15 simulations of the MESH hydrological model to allow assessment of uncertainty for flow simulations, as well as characterizing the uncertainty in streamflow probabilities for the Bow and Elbow Rivers at Calgary. This technique was also used to estimate the changing probabilities of extreme precipitation events for the Calgary urban area to estimate local flooding potential and its change over the 21st century.

2. Study Area and Data

2.1 Study area

The Bow River Basin and the Elbow River Basin above the city of Calgary have an area of 9116 km² with elevations ranging from 1025 to 3459 m.a.s.l. The Upper Bow River Basin at Banff has an area of 2210 km² with elevations ranging from 1376 to 3455 m.a.s.l. The Elbow River Basin at Sarcee has an area of 1190 km² with elevations ranging from 1054 to 3065 m.a.s.l. The Elbow River joins the Bow River in the city of Calgary and their combined flows form the Bow River which later joins the Oldman River to create the South Saskatchewan River. Due to the large variation in elevation within the basins above Calgary, a correspondingly large spatial variability is found in the precipitation from the ridge of the mountain towards the valley at seasonal and monthly scales. The majority of the precipitation in the basin is derived from convection events (in summer) and frontal events (in winter), which include persistent westerly storms and periodic heavy precipitation upslope events that focus on the Front Ranges (Whitfield & Pomeroy, 2016).

2.2 Data

2.2.1 WRF-ERA40 and WRF-PGW modelling

The Global Water Futures core modelling group, in collaboration with the US National Center for Atmospheric Research (NCAR), has developed a high resolution (~4km) regional climate model using WRF to simulate the historical and future climates of western Canada. The model has been used to produce climate simulations for two time periods: a) for the recent historical (2000-2015) period, forced by the ERA-Interim reanalysis data and b) for a future (2085-2100) period, as a PGW scenario obtained by adding climate change signals to the ERA-Interim modelled reanalysis data (Li et al., 2019). The climate change signals are derived from the CMIP5 multi-model ensemble mean (19 ensemble members) under the RCP8.5 scenario from 2071–2100 relative to 1976–2005 (Rasmussen et al., 2011, 2014). The high resolution WRF regional simulation uses convection-permitting models, which explicitly represent the fine-scale weather processes critical for simulating convective precipitation. From a hydrological perspective, these fine resolution simulations are required to model precipitation and runoff generation mechanisms for the complex terrain in mountains. Complex terrain has a large spatial variability in forcings, particularly of precipitation, due to the large differences in surface elevation over small distances

2.2.2 CanRCM4 data

The NA-CORDEX (North America – Coordinated Regional Downscaling Experiment) has developed regional climate models to run over a domain covering most of North America using boundary conditions from global climate model (GCM) simulations in the CMIP5 archive (Whan et al., 2016; Whan & Zwiers, 2016). The Climate Modelling and Analysis (CCCma) model has the same dynamical core as the Global Environmental Multiscale (GEM) model, which is an integrated numerical weather forecasting and data assimilation system developed by ECCC (Côté et al., 1998). CanRCM4 uses the same package of physical parameterizations with the fourth-generation Canadian atmospheric global climate model (CanAM4) of CCCma (von Salzen et al., 2013), which forms the atmospheric component of CanESM2 (Canadian Earth System Model 2). CanRCM4 uses the deep-convection scheme of Zhang and McFarlane (1995), a shallow-convection scheme following von Salzen et al. (2005), and the Canadian Land Surface Scheme version 2.7 (Verseghy, 2012). Scinocca et al. (2016) provide further details of the main characteristics and physical parameterizations of this RCM and its relationship with its parent global model CanESM2.

This study retrieved 15 members of the 0.44 degrees resolution product CanRCM4 at 3- hour time step under the RCP8.5 scenario. The 15 simulations share the same spatial boundary conditions, differing only in the initial conditions at the beginning of the historical simulation period. The choice of the number of ensembles examined is based solely on publicly available data at the time of this analysis, but is felt to represent the full range of RCM behaviour in the original ensemble (Asong et al., 2010). RCP8.5 is a high-emission scenario corresponding to radiative forcing of 8.5 W m^{-2} by the end of the 21st century, as compared to pre-industrial values (IPCC, 2013); therefore, it is an appropriate scenario for business-as-usual and lack of effective global climate policy. Moreover, RCP 8.5 has closely matched recent emissions

(Sanford et al., 2014). From each simulation, 3-hourly temperatures at the surface (2 m) and three upper levels (i.e., 500, 850 and 1000 hPa), surface air pressure, precipitation, and surface (10 m) wind speeds are used to calculate 3-hourly freezing precipitation (FP) and ice accretion.

Only the uncertainty due to the projected changes in precipitation is analyzed in this project. As the spatial resolution of the CanRCM4 forcing data is large, the simulations are bias-corrected, down-scaled and perturbed by the WFDEI-GEM-CaPA dataset. The WFDEI-GEM-CaPA product was obtained by merging the EU WATCH ERA-Interim reanalysis (WFDEI) data (Weedon et al., 2011) which has a long historical record (~50 years) and the meteorology from the Global Environmental Multiscale (GEM) atmospheric model along with Canadian Precipitation Analysis (CaPA) system. The final 15 CanRCM4 simulations have a spatial resolution of approximately 10 km, and provide both current climate and the RCP 8.5 scenario.

3. Methodology

3.1 Using the CanRCM4 precipitation frequency distributions to perturb WRF precipitation fields

The simplest formulations of bias correction only change a specific statistical aspect (often the change in the mean value or the variance) of the simulated fields, which is equivalent to correcting the observations with an additive or multiplicative gridded constant, called as a change factor. However, this technique is not effective for precipitation due to the intermittency (i.e. the presence of zero values) in the data sets. Quantile mapping, where simulated quantiles are mapped to the observed quantiles, has proven useful in case for precipitation (Cannon et al., 2015). Typically, a probability distribution is fitted to the observed data (here WRF) and simulated data (here CanRCM4). A given simulated value x_s at time t is mapped by using the transfer function defined as:

$$\hat{x}_s(t) = F_o^{-1} \left(F_m(x_s(t)) \right) \quad (1)$$

where F_o and F_s are the cumulative distribution function (CDF) of the observed (o) and simulated (s) data respectively. The efficiency of this method depends on how well the probability distributions fits the data.

After investigating several distributions, it was noted that the Log-normal distribution fits reasonably well to the WRF precipitation data for all months. However, the CanRCM4 outputs are not modelled well by any probability distributions for some particular months. The monthly CanRCM4 data often shows an irregular behaviour, with a sudden fall in exceedance probabilities, particularly at large values. Figure 1 plots an example—the exceedance probabilities for 2 months of precipitation rates (mm/3-hr) at a particular grid cell with two cases. In case (1) the WRF and one simulation # r8i2p1r1 of CanRCM4 are fitted well by log-normal distributions for both WRF and CanRCM4 r8i2p1r1, and the quantile mapping works well to reproduce WRF characteristics. In case (2) the log-normal

distribution fits well for WRF and poorly for the CanRCM4 simulation, causing the quantile mapping to reproduce unrealistic values. Unfortunately most of the cells in some months of the CanRCM4 simulations have similar results. We therefore modified the quantile mapping method. Instead of fitting a distribution to the CanRCM4 simulations, only the spatial patterns of the precipitation, which evolve due to the advection and/or convection processes, were retained.

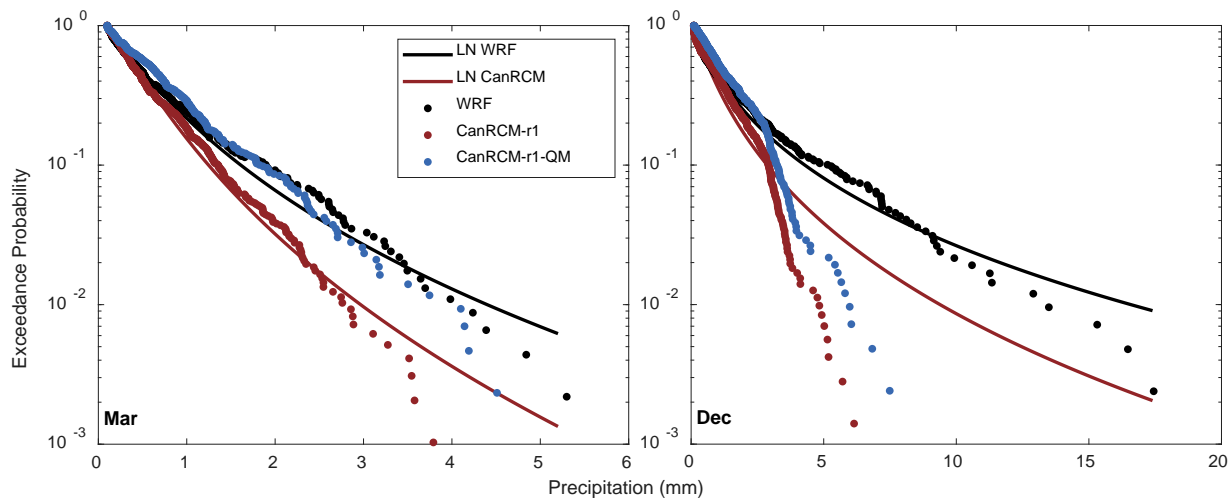


Figure 1. Exceedance probability of precipitation rate (mm/3-hr) at one grid cell for WRF data (black dots), fitted log-normal distribution to WRF data (black line), CanRCM4 r8i2p1r1 simulation (red dots), the fitted log-normal distribution to the CanRCM4 simulation (red line), and the quantile mapped (QM) precipitation of the CanRCM4 simulation (green dots).

The modified method is as follows, for each grid cell and each month

1. random numbers are generated using the log-normal distribution fitted to the non-zero precipitation data of WRF for that month,
2. the non-zero precipitation values of the CanRCM4 simulation are ranked and
3. the values of CanRCM4 are replaced with the generated random numbers according to their ranks.

In the case where the number of dry days from WRF is greater than that of CanRCM4, the lowest ranked ($n - m$) values are considered as zero, where n and m are the number of non-zero precipitation values in the WRF run and CanRCM4 simulations, respectively. In cases where the predicted number of dry days from WRF is less than that of CanRCM4, the probability of dry days from CanRCM4 is retained. With this procedure the spatial patterns of the CanRCM4 are retained (i.e., a small value in CanRCM4 simulation is still a small value, and a dry day in the simulation is still a dry day), and the adjusted precipitation values follow the log-normal distributions with parameters estimated from WRF.

3.2 Frequency analysis of precipitation at Calgary

Frequency analyses are often performed for important practical applications such as hydrological risk analysis and design of hydraulic structures. Intensity Duration Frequency (IDF) curves are commonly used in engineering practice as a part of risk analysis. IDF curves are simple functions between the precipitation intensity i , the timescale d at which the precipitation process is studied, and the return period T (or the frequency, $1/T$). Typically, a probability distribution, $F_{I(d)}$, is fitted to the tail sample of a given timescale, and the precipitation intensity for a return period is estimated by inverting the cumulative distribution function or CDF (i.e., the quantile function of the distribution):

$$i(d, T) = F_{I(d)}^{-1} \left(1 - \frac{1}{T} \right) = Q_{I(d)}(T) \quad (2)$$

Alternatively, empirical forms of the IDF curve are also popularly used due to their simplicity and because their parameters are easy to estimate for most simple forms. In this report, both the approaches are used to obtain the IDF curves for Calgary, i.e., 1) fitted distributions and 2) empirical equations. In the first approach, Gumbel frequency distributions are fitted to the annual maxima time series for different durations ($d = 3, 6, 12, 24$ and 48 hours) and the location and scale parameters of the distribution determined as shown in Table 1. The precipitation intensities for the return periods can then be obtained from the quantile function of the Gumbel distribution. In the second approach, a simple empirical equation is used (Grimaldi et al., 2011):

$$i(d, T) = \frac{aT^\beta}{(d^\gamma + \delta)} \quad (3)$$

where a, β, γ, δ are empirical parameters, whose values are estimated by minimizing the mean square error between the values of the given data and the corresponding values from Equation (3). Table 2 gives the values of the parameters of the empirical equation for the WRF-PGW and WRF-CTL (WRF control) datasets. The observed intensities are plotted with the calculated values from both datasets in (Figure 2). From the figure, it is evident that both the Gumbel and the empirical equations fit the observed points equally well to the observed points; although, the Gumbel distribution may underestimate the precipitation for high large return periods. Also, for short durations, the empirical equation is consistent with the observed precipitation intensities. Therefore, the empirical equation is chosen for developing the IDF curves. It is worth noting that empirical equation is more parsimonious, with only four parameters, than the Gumbel. The Gumbel equation requires 10 parameters to be estimated for each duration under consideration.

Table 1. Gumbel parameters for IDF curves from WRF-CTL (current climate and WRF-PGW (future climate) model runs

Run	Duration, d (hr)	Location	Scale
WRF-CTL	3	5.368	1.538
	6	3.411	0.872
	12	2.012	0.531
	24	1.350	0.362
	48	0.849	0.187
WRF-PGW	3	7.298	4.083
	6	4.593	2.571
	12	2.680	1.322
	24	1.709	0.865
	48	1.090	0.389

Table 2. Parameters of empirical equation to predict IDF curves for WRF-CTL and WRF-PGW runs

Run	α	β	γ	δ
WRF-CTL	9.135	0.346	0.670	8.0E-06
WRF-PGW	11.978	0.517	0.707	3.5E-06

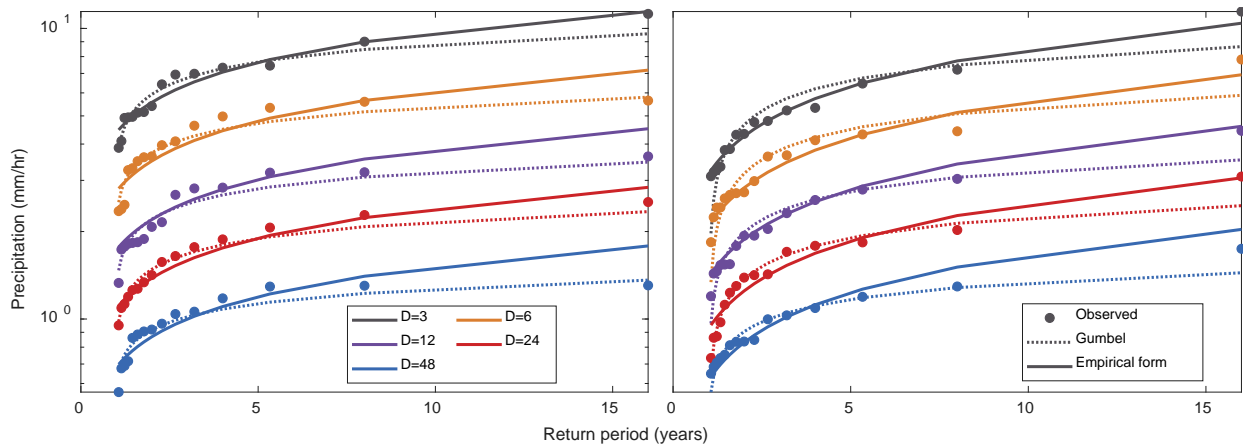


Figure 2. Observed (dots) precipitation rates (mm/hr) (according to the empirical distribution function using Weibull plotting position), precipitation rates obtained from Gumbel distribution (dashed lines) and from empirical form of IDF curve (solid lines) for different durations and return periods.

3.3 MESH runs using historical WRF and CanRCM4 perturbed WRF-PGW

The MESH model couples the Canadian Land Surface Scheme (CLASS) and the WATROFF flow routing model. The hydrologic response model of MESH is a blend of vertical mass and energy flux equations from CLASS and lateral water flux equations and concepts from WATFLOOD and elsewhere. The vertical flux equations of CLASS are much more physically based than in most hydrological models and include the necessary cold regions processes such as blowing snow, frozen soil infiltration, slope/aspect effects on the radiation balance, evapotranspiration, sublimation and glacier melt. Manning's equation is used to calculate the outflow of the assumed stream network in each grid. Within each grid cell, the water level is assumed to be constant and channels are assumed to be rectangular with sloping sides for the floodplain. The model also simulated the water management processes needed to simulate the reservoir- managed river hydrographs in the basin. The version of MESH used here is termed "Mountain MESH", which is an improved representation of slope, aspect and topography. The modelling domain covers the Bow and Elbow River basins above Calgary but for the calibration, flows of the Bow River Basin at Banff and the Elbow River Basin at Sarcee Bridge were used. The basin model included shown in Figure 3.

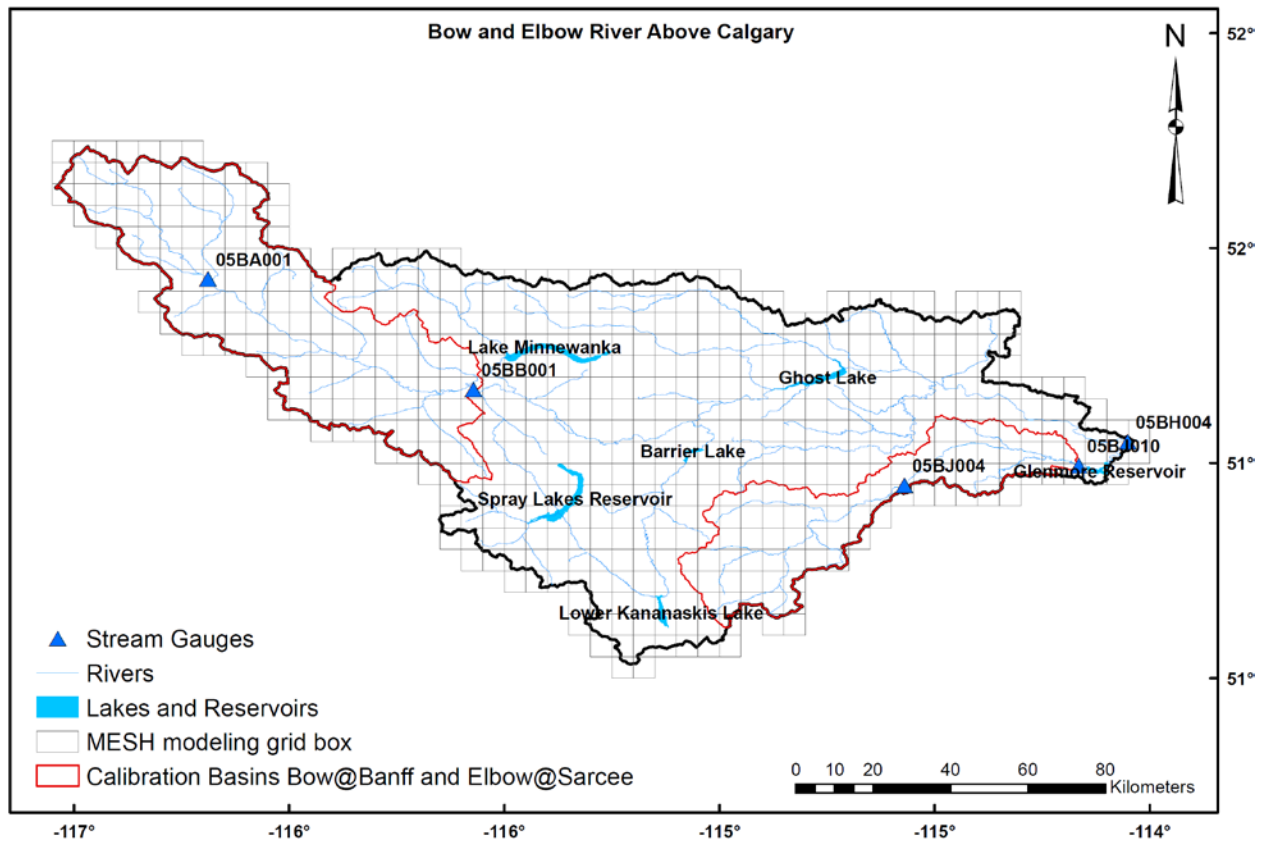


Figure 3. Bow and Elbow River Basins above Calgary: river network, and reservoirs, shown with the 4 km model grid.

The calibrated and validated MESH model developed for the BRBS was used to simulate streamflows using the historical period (2001 – 2015) and pseudo global warming (2086 – 2100) forcings. The model parameters from the calibrated MESH hydrological model were transferred to the entire basin Bow and Elbow River Basins above Calgary. The WRF-PGW (with all seven sets of climate forcings) and the output from CanRCM4-based perturbed WRF-PGW precipitation fields were used to drive the calibrated hydrological model to produce simulated future streamflows and their uncertainties.

Daily simulated streamflows were corrected using a quantile - quantile mapping approach that avoided the highly uncertain correction of the WRF simulated climate forcing, but instead using the more certain daily streamflow data from four Water Survey of Canada gauging stations in the basin. Following the Gudmundsson et al., (2012) statistical bias correction recommendation showed that the nonparametric transformations not only have the best skill in reducing biases from climate data through the entire range of the distribution, but also and can be applied without making specific assumptions about the distributions of the data. Moreover, there is R package (Statistical Transformations for Post-processing Climate Model: qmap) that was used available to bias correct the simulated streamflow. The bias correction using the Quantile Mapping (QM) approach was parameterized with the observed daily streamflow data and historical simulated MESH-WRF for the historical calibration period (2001 – 2015) and was then used correct both the future

MESH-WRF-PGW and CanRCM4-WRF-PGW simulated streamflows. Quantifying uncertainty in the streamflow is not possible with the WRF data as only a single model run is currently available. Therefore, the variability in the CanRCM4 simulations was utilized to perturb the WRF PGW run using the novel method as described in section 3.1. The flow duration curves of the four gauging stations were produced from the bias-corrected simulated streamflows observations, WRF and CanRCM4-WRF-PGW MESH simulations.

4. Results

4.1 WRF-Historical and WRF-PGW Meteorology

Precipitation varies considerably from month to month in the WRF-PGW simulation with large seasonal variability. The monthly statistics of precipitation rate (mm/3-hr) in Table 3 show that the wettest months are the summer months (June, July and August) – a period with large seasonal variability in precipitation. Spatially, high monthly precipitation rates are found in the plains during summer and in the mountains during winter months (Figure 4). The probability of dry days is large in the mountains during the summer (Figure 5).

Table 3. Statistics of precipitation (mm/3-hr) for WRF-PGW (SD=standard deviation, Q=quantile)

Stats	Jan	Feb	Mar	Apr	May	Jun	Jul	Aug	Sep	Oct	Nov	Dec
Mean	1.13	0.93	1.16	1.29	1.67	2.24	2.28	2.19	1.64	1.20	1.28	0.99
SD	1.53	1.26	1.56	1.76	2.41	3.21	3.83	3.71	2.47	1.78	1.76	1.36
Max	29.94	26.76	50.28	31.53	63.58	76.60	84.36	103.76	67.14	42.40	37.76	33.39
Q_5	0.12	0.12	0.12	0.12	0.13	0.13	0.12	0.12	0.12	0.12	0.12	0.12
Q_{25}	0.25	0.21	0.24	0.26	0.29	0.35	0.29	0.29	0.26	0.24	0.26	0.23
Median	0.57	0.46	0.57	0.63	0.76	1.00	0.83	0.80	0.70	0.56	0.62	0.49
Q_{75}	1.34	1.11	1.42	1.57	2.04	2.79	2.54	2.45	1.95	1.41	1.54	1.18
Q_{95}	4.10	3.31	4.16	4.70	6.26	8.44	9.50	8.95	6.37	4.44	4.64	3.52

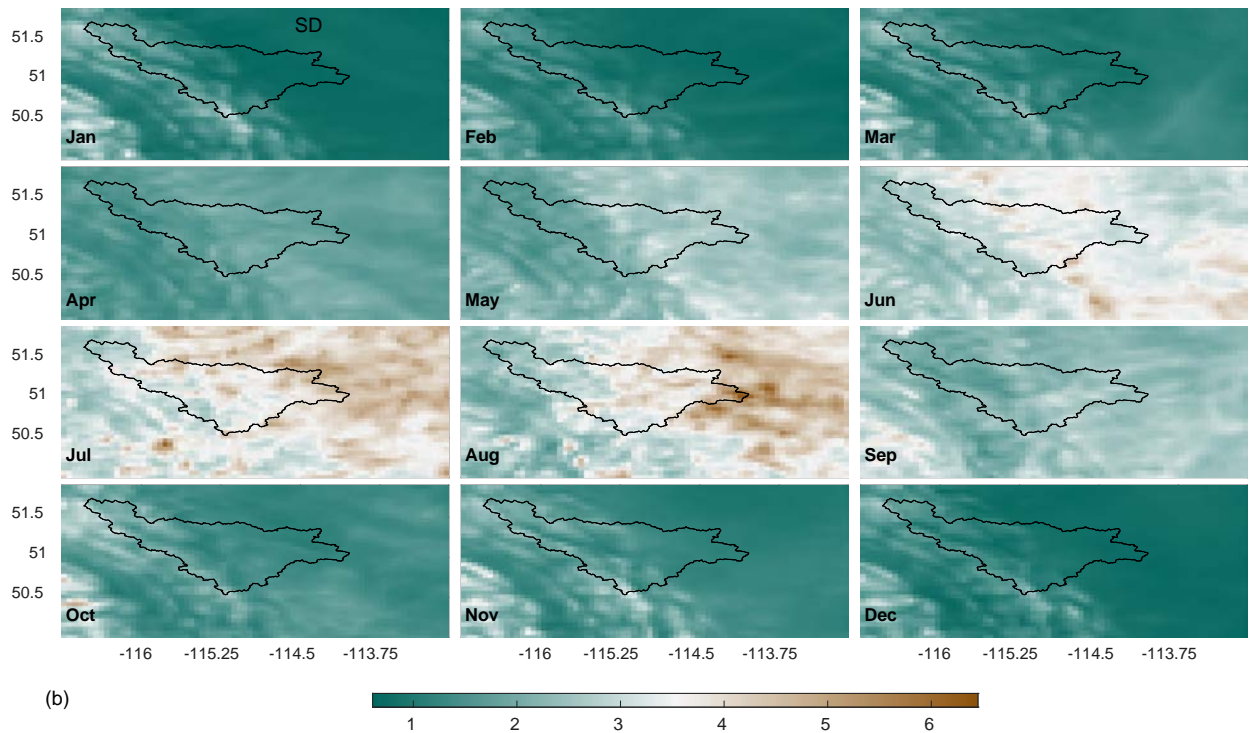
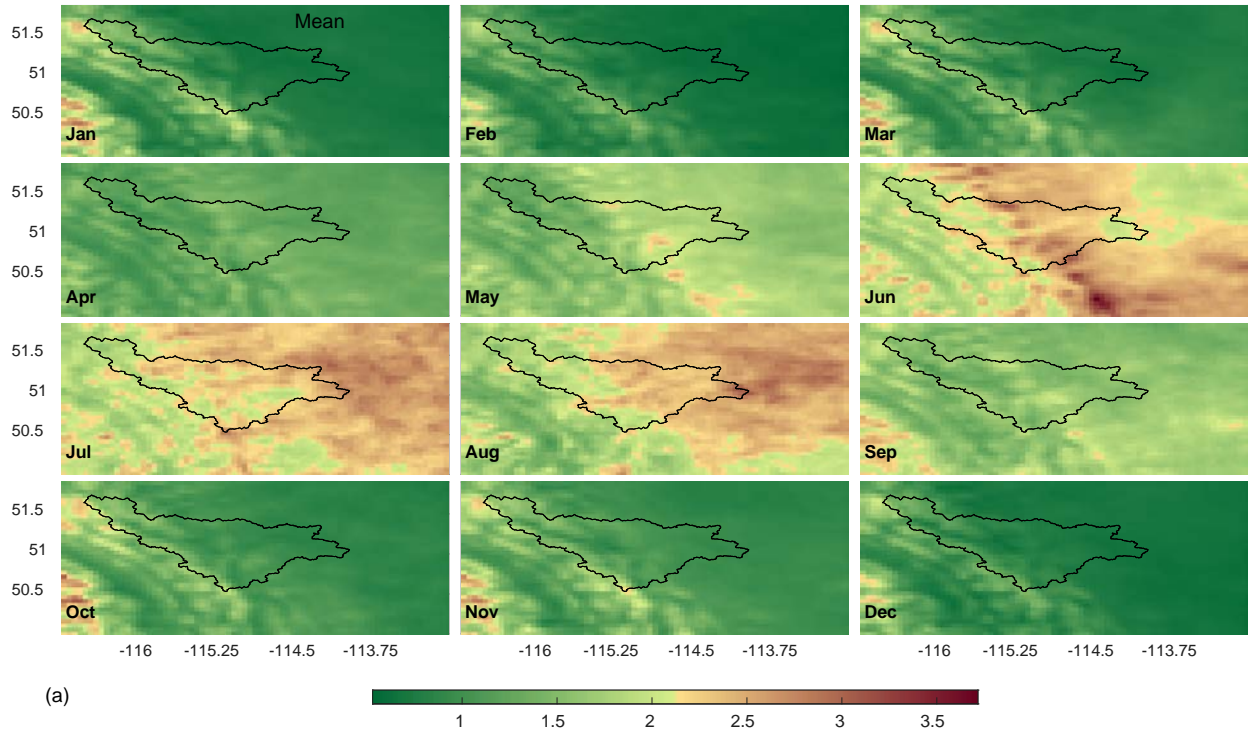


Figure 4. Spatial variation of (a) mean and (b) standard deviation of precipitation rate (mm/3-hr) from WRF-PGW. Axes are latitude on y and longitude on x axis respectively. Pseudo-Global Warming (PGW) is for 2085-2100.

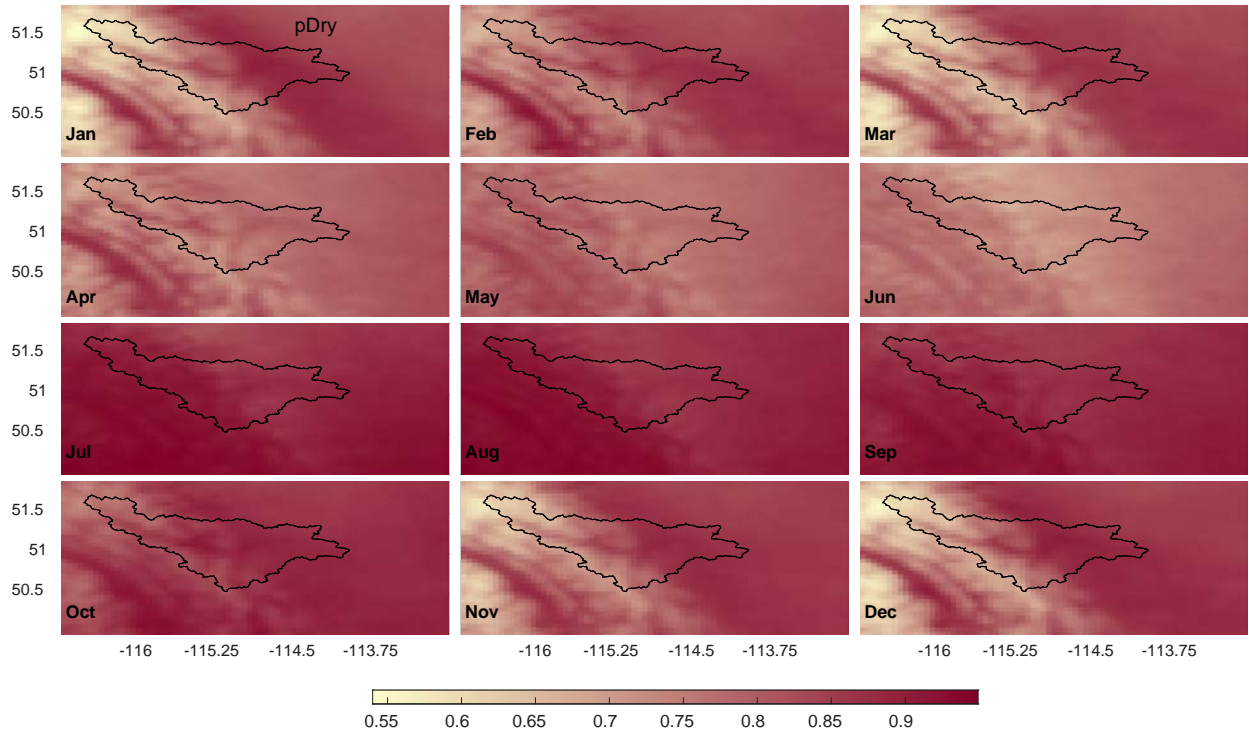


Figure 5. Spatial variation of the probability of dry days from WRF-PGW. Axes are latitude on y and longitude on x axis respectively. Pseudo-Global Warming (PGW) is for 2085-2100

4.2 CanRCM4 Meteorology

The precipitation from the 15 members of the CanRCM4 were compared with the WRF-PGW during for the period 2085-2100. Basic statistics like mean, standard deviation, and different quantiles are compared. As well, the intermittency, probability of a dry day and its spatial variability are compared. Figure 6 shows the mean and standard deviation of mean 3-hourly precipitation rates for the 15 CanRCM4 members as (box plots) for each month. The black dot represents the WRF-PGW mean. It is evident that the CanRCM4 simulations member statistics differ considerably from the WRF-PGW in most months (except December). CanRCM4 precipitation rates in the months of May and June have the greatest mean values for all members, in contrast to the WRF-PGW where high values are found in the months of June, July and August. The standard deviations show very large differences ($\sim 3\text{mm}/3\text{-hr}$) over the months of July and August. Figure 7 compares the dry day probability between WRF-PGW and CanRCM4 simulations. The dry day probability is generally large for most of the simulations and for all months. In addition to the differences between WRF and CanRCM4 datasets, there is a great spatial variation in precipitation amongst the simulations.

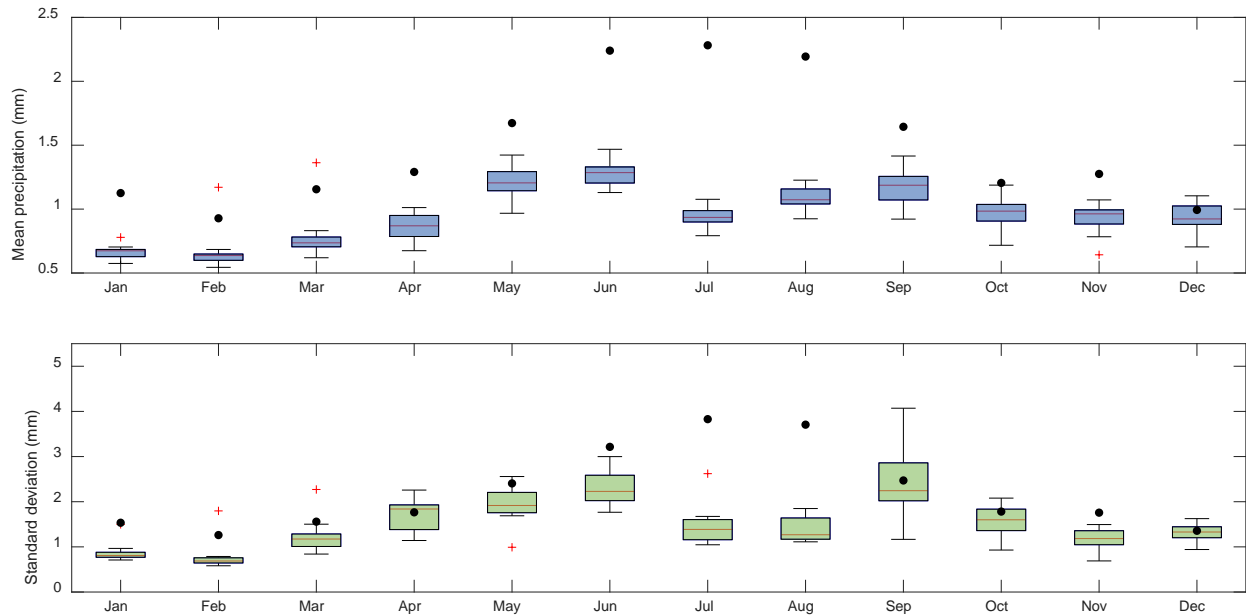


Figure 6. Comparison of mean and standard deviation of 3-hourly precipitation rates (mm/3-hr) between WRF-PGW and CanRCM4 15 simulations. Box plots show the mean precipitation rate for all simulations, black dots show the mean precipitation rate from WRF-PGW, and red plus symbols show the outliers from the CanRCM4 simulations.

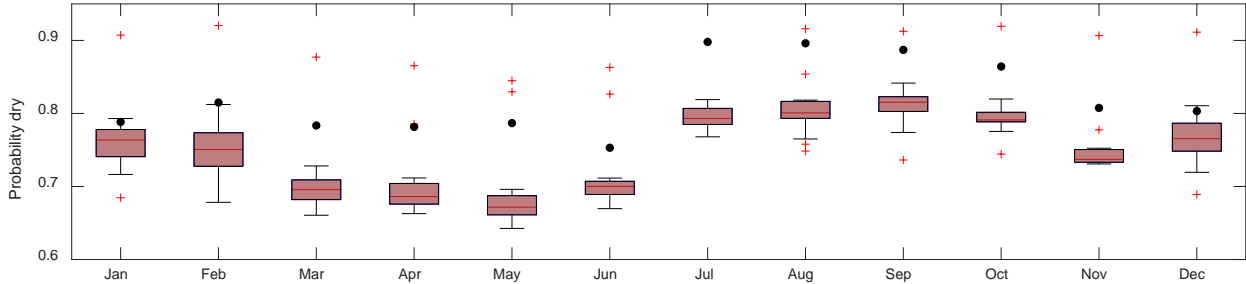


Figure 7. Comparison of the probability of dry days between WRF-PGW (black dots) and CanRCM4 15 simulations. Box plots show the mean probability of dry days for all simulations, and red plus symbols show the outliers from the CanRCM4 simulations.

4.3 CanRCM4 perturbed WRF-PGW Meteorology

Each CanRCM4 simulation was perturbed using the log-normal distribution fitted to the WRF-PGW, retaining the spatial patterns of the simulation. Figure 8 shows the spatial pattern of evolution of a storm in the study area. The mean and standard deviation of the corrected simulations' precipitation largely match those of WRF-PGW. Figure 9 shows the histograms of mean and standard deviation of precipitation rate (mm/3-hr) at all grids in the study area for the WRF-PGW and one CanRCM4 simulation (r8i2pir1), both the original and bias corrected, and Figure 10 shows histograms of the probability of dry days (# of dry days/# of days). It is notable that, after correcting, most of the values of the statistics (mean,

standard deviation, L-variance, L-skewness L-kurtosis) for the perturbed CanRCM4 outputs, match those of the WRF-PGW.

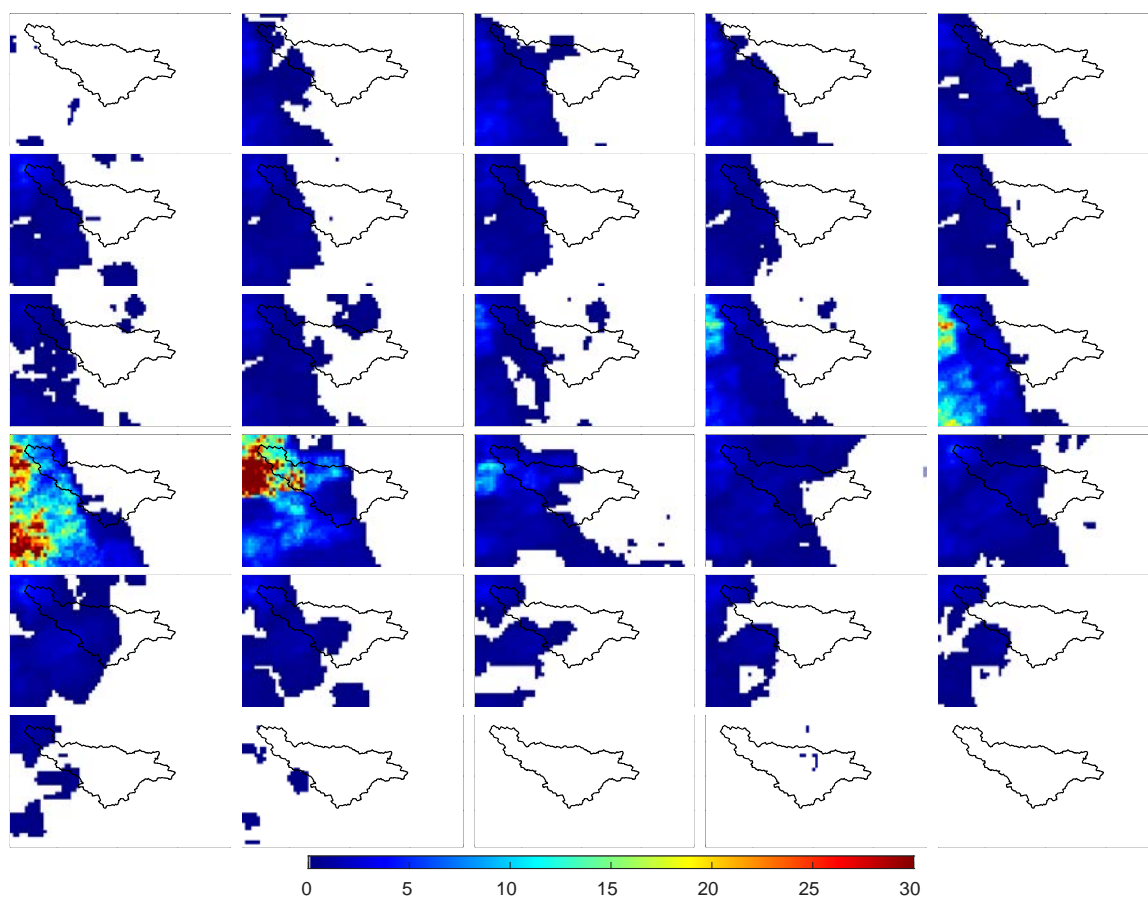


Figure 8. Evolution of a precipitation event in the bias corrected CanRCM4 simulation. Units for the precipitation rates shown are mm/3-hr.

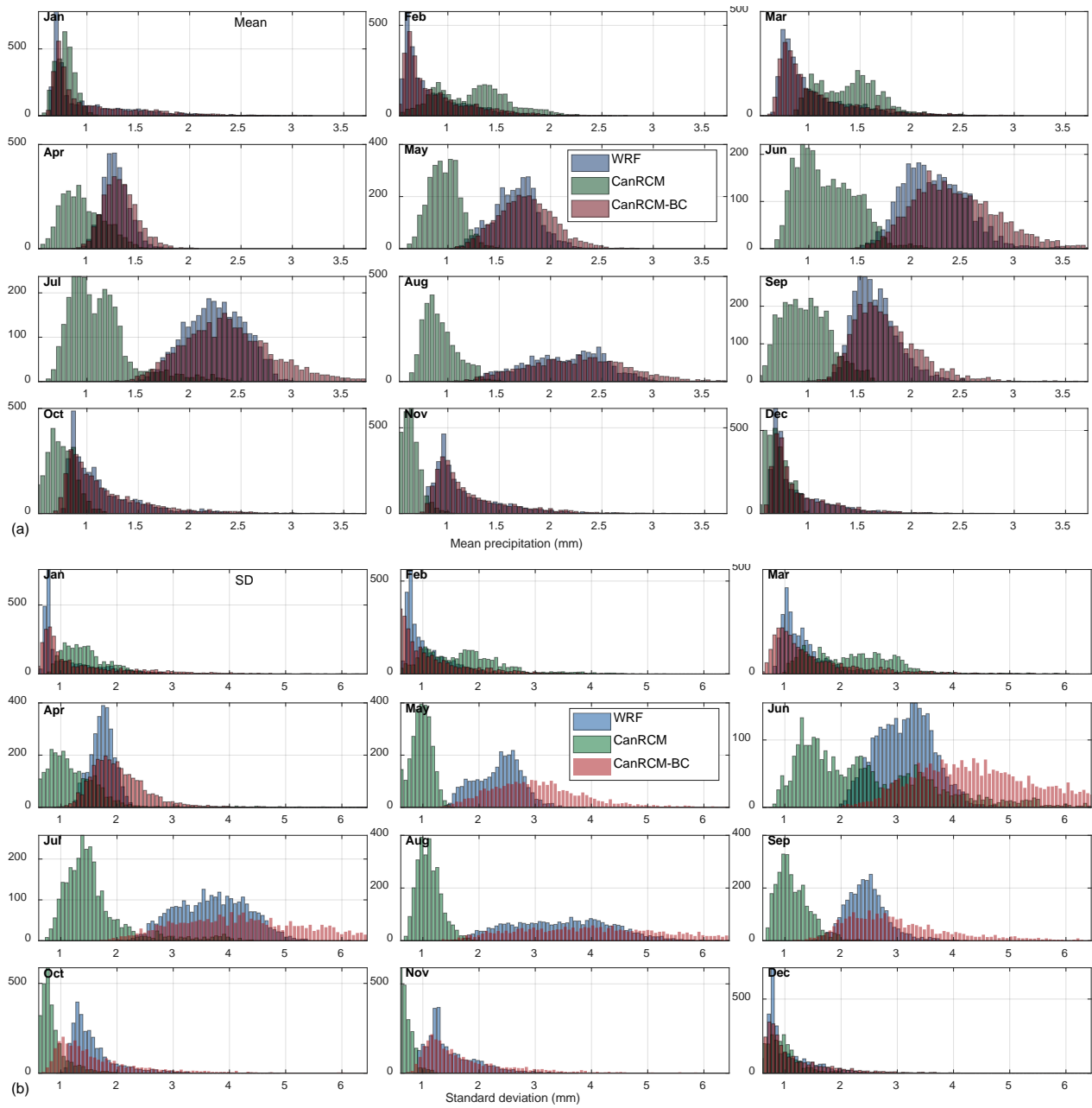


Figure 9. Histograms of mean and standard deviation of precipitation rates (mm/3-hr) of WRF-PGW (WRF), CanRCM4 simulation # r8i2p1r1 (CanRCM) and the bias-corrected values of r8i2p1r1 (CanRCM-BC).

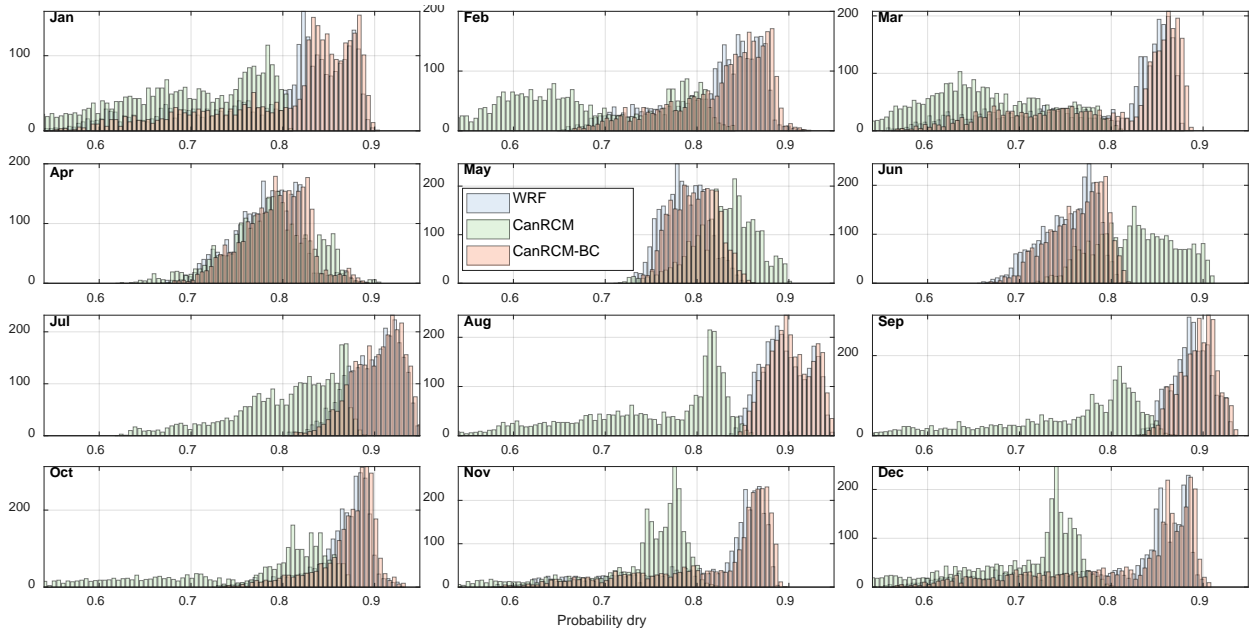


Figure 10. Histograms of probability of dry days from WRF-PGW (WRF), CanRCM4 simulation # r8i2p1r1 (CanRCM) and the bias corrected values of r8i2p1r1 (CanRCM-BC).

4.4 Change in extreme precipitation at Calgary

Extreme precipitation rates at Calgary increased from WRF-CTL to WF-PGW. Table 5 shows the percentage increase $(PGW - CTL)/CTL \times 100$ in precipitation rates (mm/hr) for various durations and return periods. Increases of up to 55% were found for short return periods ($T=2, 5$), and an increase of 300% for large return periods ($T=500, 1000$). The IDF curves were developed for the 15 CanRCM4 perturbed simulations for obtaining the uncertainty range. Table 4 shows the parameters of the empirical form of the IDF curve for the CanRCM4 perturbed simulations. Figure 11 shows the IDF curves for different various return periods. As expected, the uncertainty range in the CanRCM4 simulations increase as the return periods increase.

Table 4. Percentage increase in precipitation intensity (mm/hr) from WRF-CTL to WRF-PGW for different various durations, d (hours) and return periods, T (years).

Return period T	Duration, d , (hours)				
	3	6	12	24	48
2	41.7	38.1	34.7	31.3	28.0
5	65.7	61.5	57.4	53.5	49.6
10	86.4	81.7	77.2	72.7	68.3
25	117.9	112.4	107.1	101.9	96.8
50	145.3	139.1	133.1	127.2	121.5
100	176.0	169.0	162.3	155.7	149.2
500	263.1	253.9	245.0	236.3	227.9
1000	308.6	298.3	288.3	278.5	269.0

Table 5. Parameters of the empirical IDF for CanRCM4 simulations

CanRCM4 Simulation #	α	β	γ	δ
r10i2p1r1	19.85	0.61	0.87	0.61
r10i2p1r2	25.03	0.34	0.81	0.50
r10i2p1r3	59.96	0.63	1.07	3.74
r10i2p1r4	22.03	0.67	0.96	2.11
r10i2p1r5	20.80	0.67	0.89	0.95
r8i2p1r1	20.51	0.71	0.88	1.3E-06
r8i2p1r2	36.18	0.68	1.01	2.10
r8i2p1r3	54.81	0.53	1.06	4.67
r8i2p1r4	43.44	0.65	1.11	5.17
r8i2p1r5	25.63	0.63	0.92	1.24
r9i2p1r1	32.52	0.68	0.99	3.12
r9i2p1r2	27.99	0.54	0.89	0.86
r9i2p1r3	33.52	0.67	1.03	3.17
r9i2p1r4	54.45	0.63	1.06	6.10
r9i2p1r5	55.77	0.64	1.06	4.59

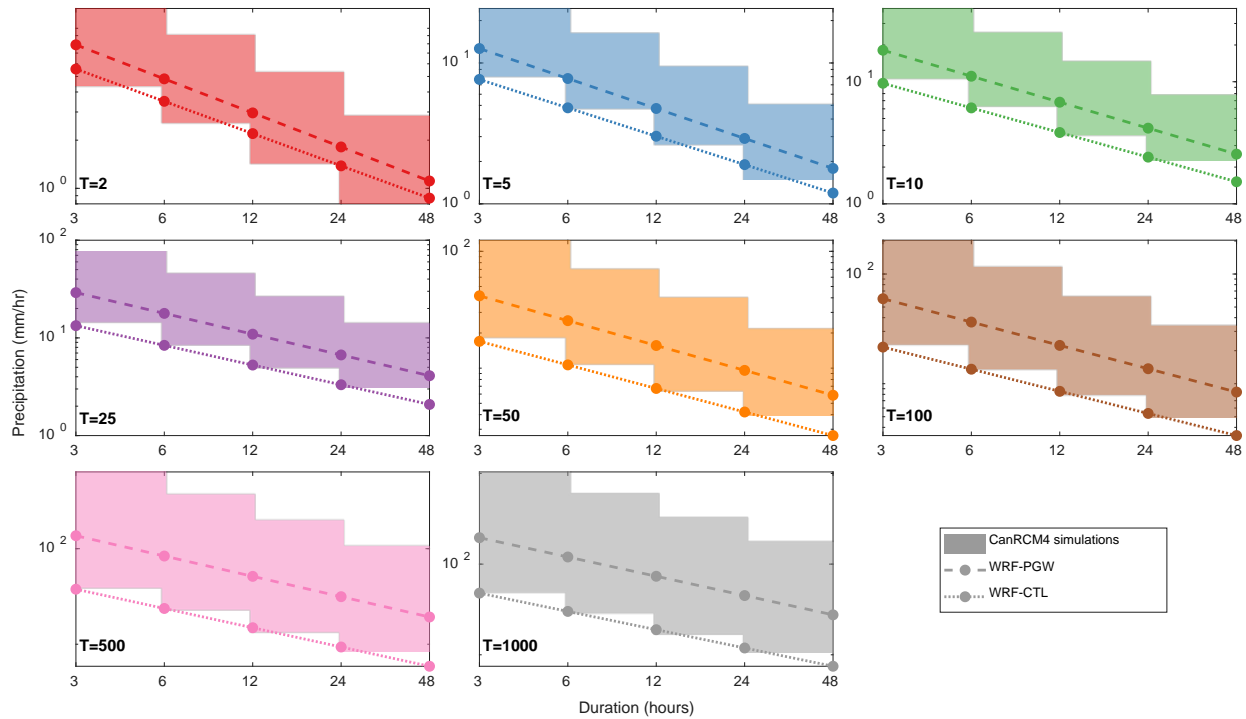


Figure 11. IDF curves for WRF-CTL (dotted lines), WRF-PGW (dashed lines) and CanRCM4 simulations for different return periods (T).

4.5 MESH driven using historical WRF meteorological forcing

Model calibrations were performed using the historical WRF meteorological forcing for the period from October, 2006 to September, 2015 and the calibration results are shown in Figure 12 for the Bow River at Banff in and Figure 13 for Elbow River at Sarcee Bridge. The calibrated hydrological model simulated the daily historical streamflow quite well with a Nash-Sutcliffe efficiency (NSE) value of 0.81, reproducing most of historical peak flows for Bow River basin at Banff. In validation, the model performance was even stronger for the Bow River at Banff (NSE = 0.87) and it was apparent that most peak flows were typically captured by the model (Figure 12).

For the Elbow River basin near Sarcee Bridge, the calibration performance was less strong than for the Bow River basin at Banff, with a NSE of 0.69. In validation, the model for Elbow River basin near Sarcee Bridge could not capture the summer rainfall-runoff events, as the magnitudes were often underestimated, and all of the snowmelt period flows were significantly overestimated with NSE of 0.5 (Figure 13).

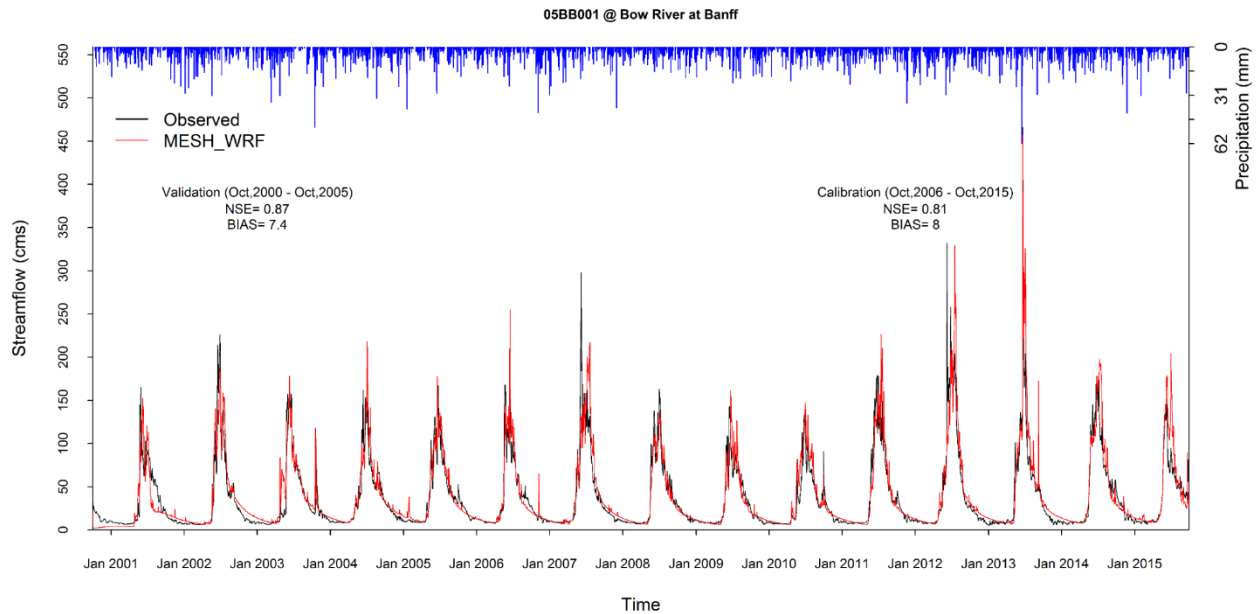


Figure 12. Calibration and validation performances for the Bow River at Banff. Streamflow is m^3/s and precipitation is mm/day .

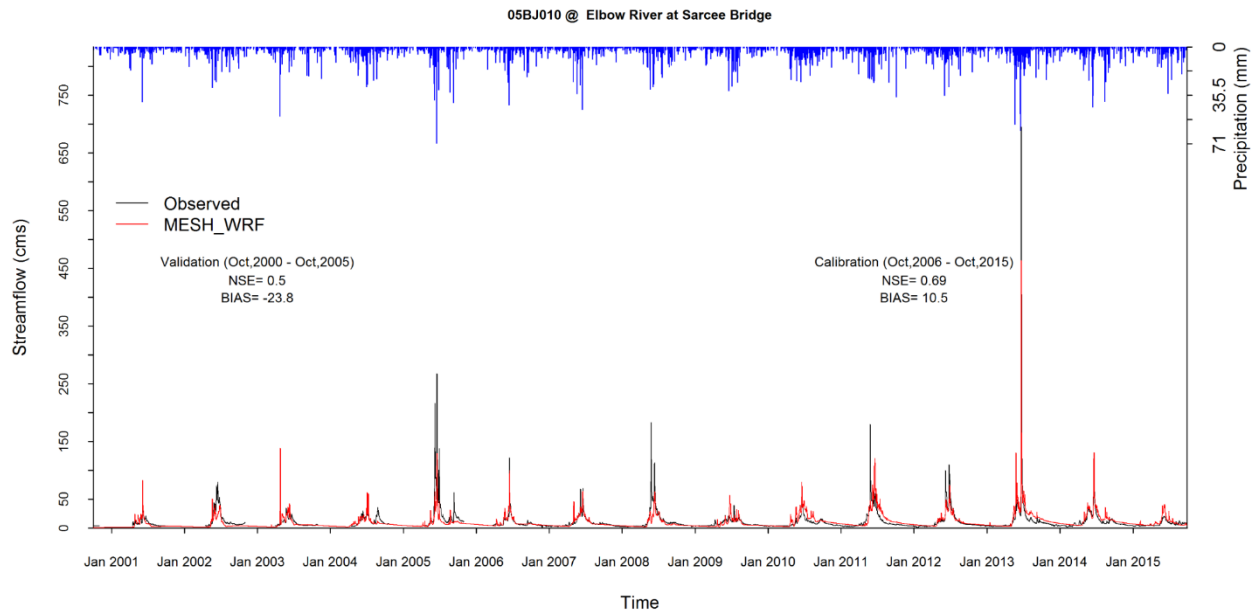


Figure 13. Calibration and validation performances for the Elbow River at Sarcee Bridge. Streamflow is m^3/s and precipitation is mm/day .

4.6 Assessment of change to extreme streamflow events using CanRCM4 uncertainty and WRF-PGW forcing data

The bias-corrected modelled (WRF-MESH and CanRCM4-WRF-PGW-MESH) flow duration curves (using the Q-Q mapping method) for the Bow River at Banff, Bow River above Calgary and Elbow River below Glenmore Reservoir are compared to those from observations in Figure 14, Figure 15, Figure 16 and Figure 17. The corrected historical modelled flow duration curve generally matched observed flow duration curve very well for the Bow River at both Banff and Calgary. Simulated low streamflows (i.e. that were exceeded 80-95% of the time) also showed good agreement with the observations; however, those that were exceeded more than 95% of the time were overestimated. This is likely due to effects of river ice in the water level measurements as those periods were flagged as ice conditions in the river by Water Survey Canada. Simulated flows smaller than the median values of the Elbow River below Glenmore Reservoir generally matched observed flow durations very well, however, the simulated high streamflows (i.e. those exceeded 5 - 55% of the time) showed underestimations, likely due to low values of heavy precipitation in the mountains of the Elbow River basin. Based on changes in the flow duration curve, median and below-median streamflows will likely increase under future climates at all gauging stations. High streamflows will have small to negligible changes. The Bow River at Calgary is strongly affected by upstream reservoirs and lakes, which were modelled in a very simple way in this exercise and it is possible that future changes to the reservoir operation rules could affect the results.

Figures 14 through 17 show the range of uncertainty in future streamflow through flow duration curve plots of the WRF and CanRCM4-WRF-PGW driven MESH model outputs. By considering multiple CanRCM4 MESH simulations, the range of uncertainty in flow duration curves under future climates was quantified. The WRF-PGW driven results suggest that future high discharge, low frequency (exceedances less than 10%) streamflows will decrease compared to current climate condition by 4, 9 and 1.6 m³/s for the Bow River at Banff and Calgary and the Elbow River at Sarcee Bridge respectively. These reductions in future low frequency streamflow are also supported by the average of the 15 CanRCM4-WRF-PGW results with which show differences in magnitude of 9, 16 and 4 m³/s for Bow River at Banff and Calgary and Elbow River at Sarcee Bridge respectively. However, there were some CanRCM4-WRF-PGW realizations that suggested substantial increases in future low-frequency streamflows as indicated by the maximum CanRCM4-WRF-PGW values as shown in Table 6 and Table 7. These increases of 60% to 250% in high flows would substantially increase flooding in the future. In contrast, future below-median and high frequency (exceedances greater than 30%) streamflows will increase in all gauging locations by from 1 to 12.5 m³/s giving a modest increase in low flow volumes.

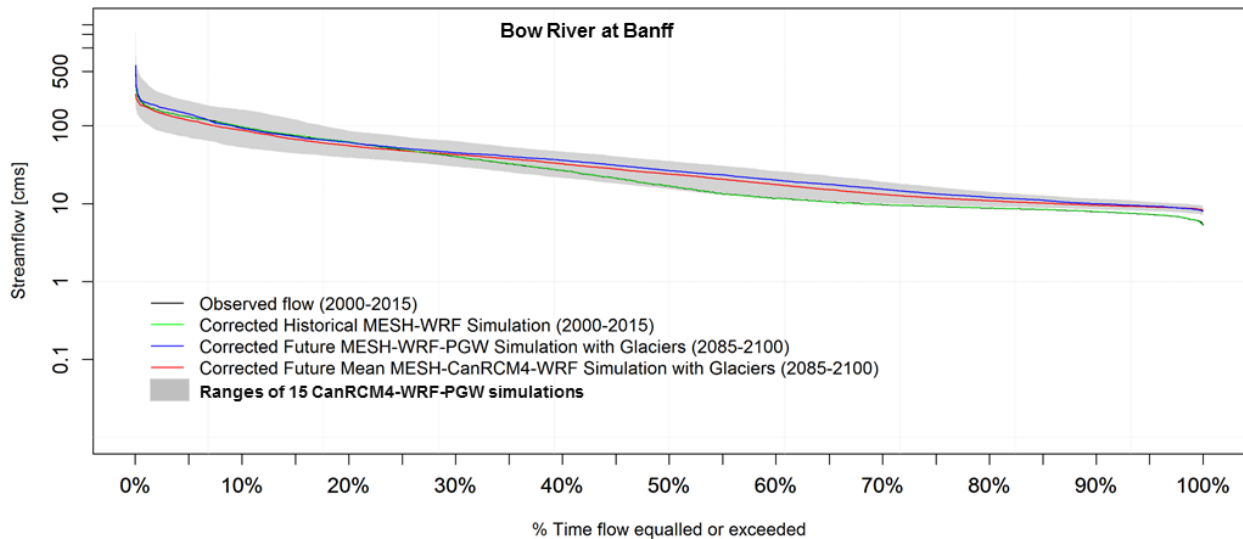


Figure 14. Simulated flow duration forced by WRF-PGW and the 15 CanRCM4-WRF-PGW for Bow River at Banff. Streamflow is in m³/s.

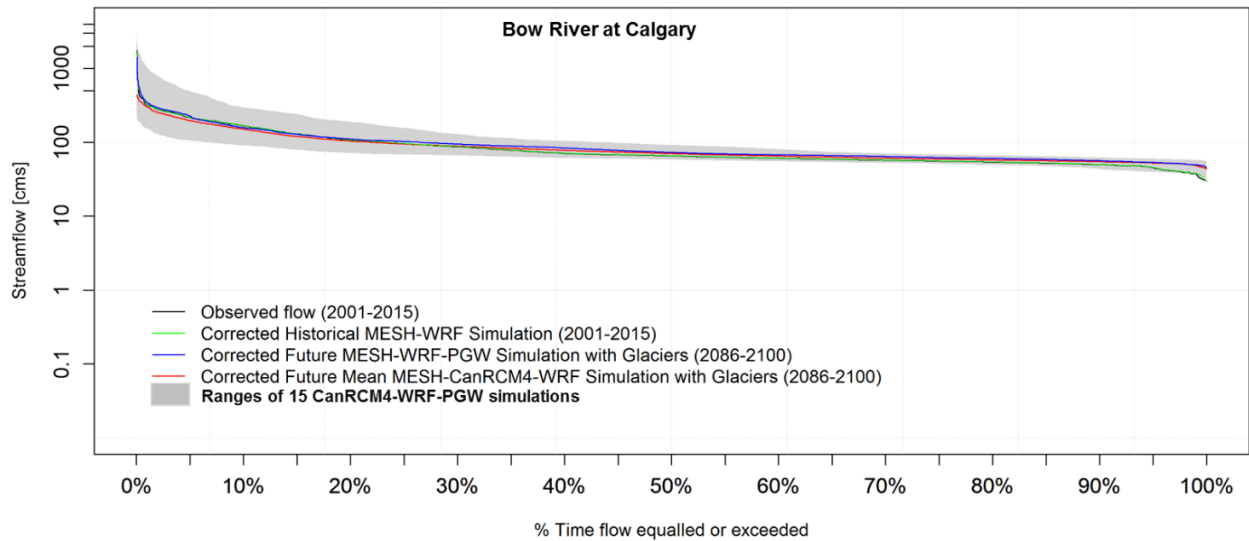


Figure 15. Simulated flow duration forced by WRF-PGW and the 15 CanRCM4-WRF-PGW for Bow River at Calgary. Streamflow is in m^3/s .

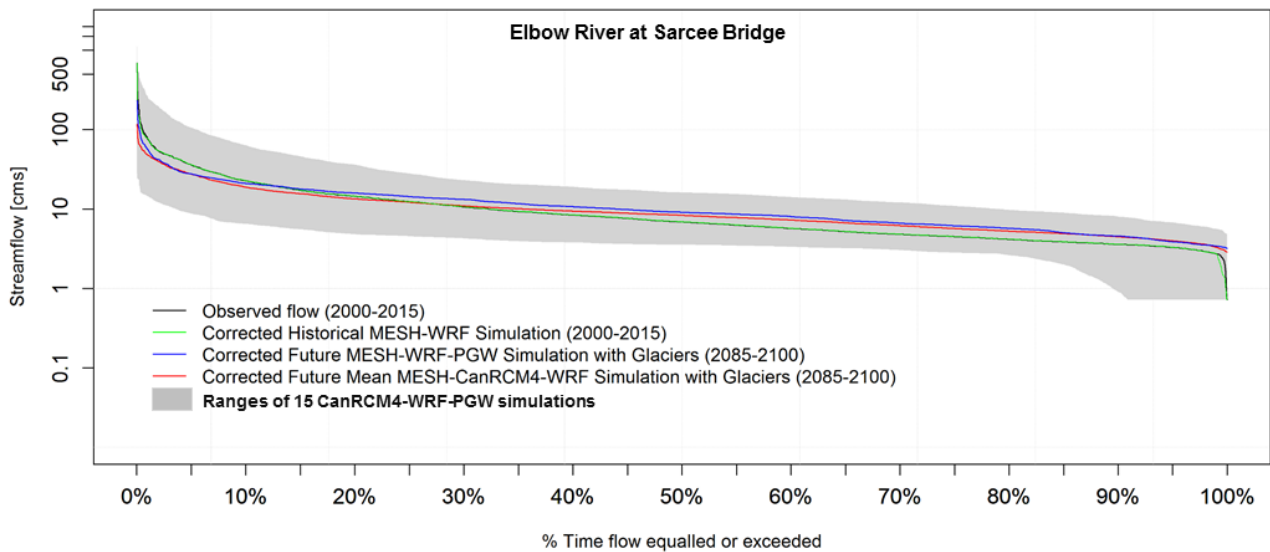


Figure 16. Simulated flow duration forced by WRF-PGW and the 15 CanRCM4-WRF-PGW for Elbow River at Sarcee Bridge. Streamflow is in m^3/s .

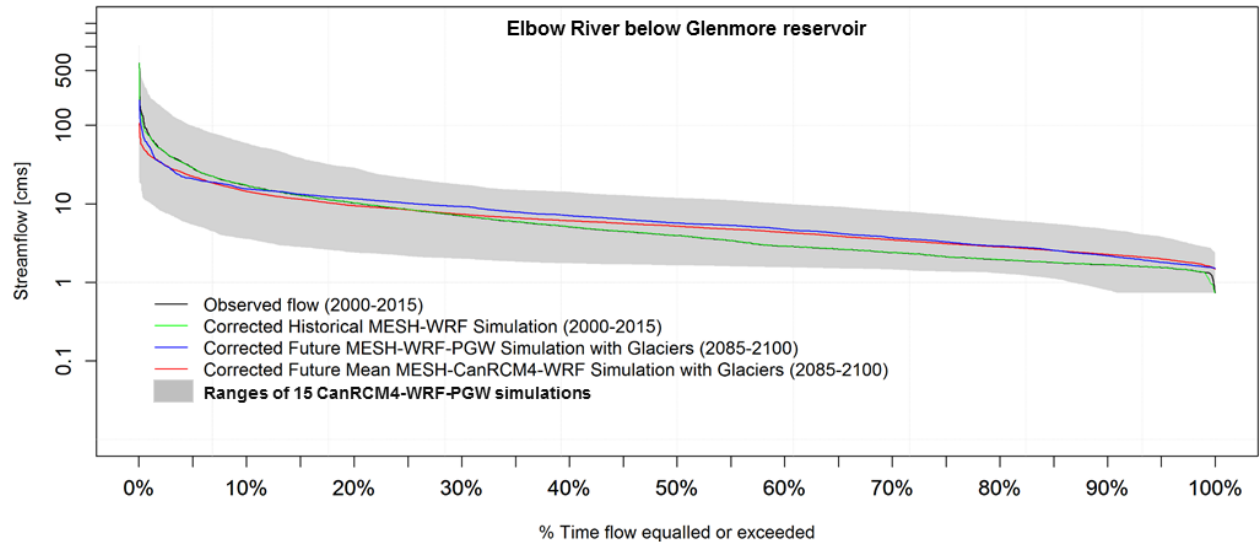


Figure 17. Simulated flow duration forced by WRF-PGW and the 15 CanRCM4-WRF-PGW for Elbow River below Glenmore Reservoir. Streamflow is in m^3/s .

Table 6. Bias-corrected historical and future-climate modelled streamflows that were exceeded 10 - 90% of the time for Bow River at Banff and Calgary. Streamflow is m³/s.

% Time Flow Equalled / Exceeded	Obs	WRF-CTL	WRF-PGW	Minimum- CanRCM4- WRF-PGW	Mean- CanRCM4- WRF-PGW	Maximum- CanRCM4- WRF-PGW
Bow River at Banff (m3/s)						
10	97.6	97.6	93.6	52.7	88.3	161.1
20	62.6	62.5	61.5	38.9	55.8	86.1
30	40.3	40.3	45.3	29.9	42.9	63.6
40	26.7	26.7	36.2	21.5	32.6	46.6
50	17.0	16.9	26.7	15.5	24.1	35.3
60	11.8	11.7	20.3	11.8	17.6	26.2
70	9.8	9.8	15.4	10.0	13.2	19.0
80	8.8	8.8	12.1	9.2	11.0	14.2
90	7.9	7.9	10.0	8.5	9.6	11.6
Bow River at Calgary (m3/s)						
10	167.9	167.1	157.8	91.1	151.3	297.6
20	107.6	107.0	110.9	71.5	104.2	188.8
30	87.6	87.5	94.6	66.4	88.9	128.9
40	71.2	71.2	83.8	61.4	78.2	104.2
50	65.8	65.7	73.2	58.3	70.6	91.8
60	61.0	60.9	67.9	55.4	65.3	80.5
70	57.6	57.5	64.5	52.6	61.2	70.4
80	54.2	54.2	60.5	49.5	57.8	66.6
90	50.0	49.9	56.4	43.3	54.7	62.1

Table 7. Bias-corrected historical and future-climate modelled streamflows that were exceeded 10 - 90% of the time for the Elbow River at Sarcee Bridge and below Glenmore. Streamflow is m³/s.

% Time Flow Equalled / Exceeded	Obs	WRF-CTL	WRF-PGW	Minimum-CanRCM4-WRF-PGW	Mean-CanRCM4-WRF-PGW	Maximum-CanRCM4-WRF-PGW
Elbow River at Sarcee Bridge (m3/s)						
10	22.7	22.7	21.1	6.5	18.9	63.5
20	14.5	14.5	16.0	4.8	13.5	36.3
30	10.7	10.7	13.3	4.3	11.0	23.0
40	8.5	8.5	10.8	3.8	9.4	19.1
50	6.9	6.9	9.2	3.6	8.4	16.2
60	5.7	5.7	8.1	3.3	7.3	14.2
70	4.8	4.8	6.7	3.1	6.2	12.1
80	4.2	4.2	5.7	2.6	5.3	9.8
90	3.6	3.6	4.6	0.9	4.5	8.0
Elbow River below Glenmore Reservoir (m3/s)						
10	17.3	17.3	15.6	3.6	14.5	59.4
20	10.3	10.3	11.7	2.4	9.5	28.8
30	7.1	7.1	9.3	2.0	7.4	17.6
40	5.1	5.1	7.1	1.7	6.1	14.2
50	4.0	4.0	5.7	1.7	5.2	11.9
60	2.9	2.9	4.7	1.6	4.3	10.0
70	2.4	2.4	3.7	1.5	3.5	8.2
80	2.0	2.0	2.9	1.3	2.8	6.3
90	1.7	1.7	2.2	0.8	2.3	4.7

5. A blueprint for calculating future streamflow discharges and their probabilities for Canada

5.1 Assessment of uncertainty in future streamflows

This study presents an uncertainty assessment scheme that can assess the impact of climate change on the streamflow frequencies using a physically based land surface hydrological model that is specially adapted for Canadian hydrology and water management and is driven by a novel climate downscaling method that uses multiple climate model realisations. Uncertainty in the future simulated streamflows for the future climate was assessed by estimating the ranges of simulated streamflow by driving the hydrological model using an ensemble of future climate realisations after they were bias-corrected to the most reliable climate model outputs.

Two sets of climate model forcings were used to drive the hydrological model in this study: high-resolution WRF and low-resolution CanRCM4. The two datasets have advantages and disadvantages. The high-resolution WRF forcing has only one realisation, which prevents it being used directly to assess uncertainty, whereas the low-resolution CanRCM4 forcing has many realisations but is too coarse spatially to be used for realistic hydrological simulations in the mountains and plains. This study developed a methodology to effectively use the advantages of both datasets by bias-correcting the low-resolution climate model outputs, then using them to perturb the high-resolution climate model output to produce several realisations of high-resolution data that could be used to force the hydrological model. The framework has been illustrated for the Bow River Basin as a real-world case study as described in the previous sections and is shown conceptually in Figure 18. The relevant contribution of this project is related to proposing and demonstrating an uncertainty estimation framework for estimating flood frequencies using novel, state-of-the-art methods.

5.2 Considerations in applying this pilot project to other basins

The methodology developed in this study to assess the effects of climate change on flood frequencies can be implemented for other studies following this blueprint. However, the uncertainty in the flow duration curve for various frequencies only used 15 future climate realizations, which somewhat limited the uncertainty analysis. We recommend expanding the number of realizations from 15 to the maximum available.

As the typical user may not be an expert in climate modelling, physically based hydrological modelling and hydroclimatological science, making decisions on hydrological model selection, downscaling and bias-correction methods for regional climate model outputs may be difficult. It would make sense to have a national set of driving meteorology for hydrological assessment of climate change impacts, developed from bias-corrected and downscaled climate models following the procedure applied here to the Bow River Basin domain. Such meteorological inputs could be used to drive MESH or other models as preferred; however the excellent experience with WRF-MESH in this basin and from ECCO studies of the Great Lakes Basin and Global Water Futures studies of the Saskatchewan,

Yukon, St John and Mackenzie river basins suggests it is the most ideal model available to apply to diagnose climate change impacts across Canada.

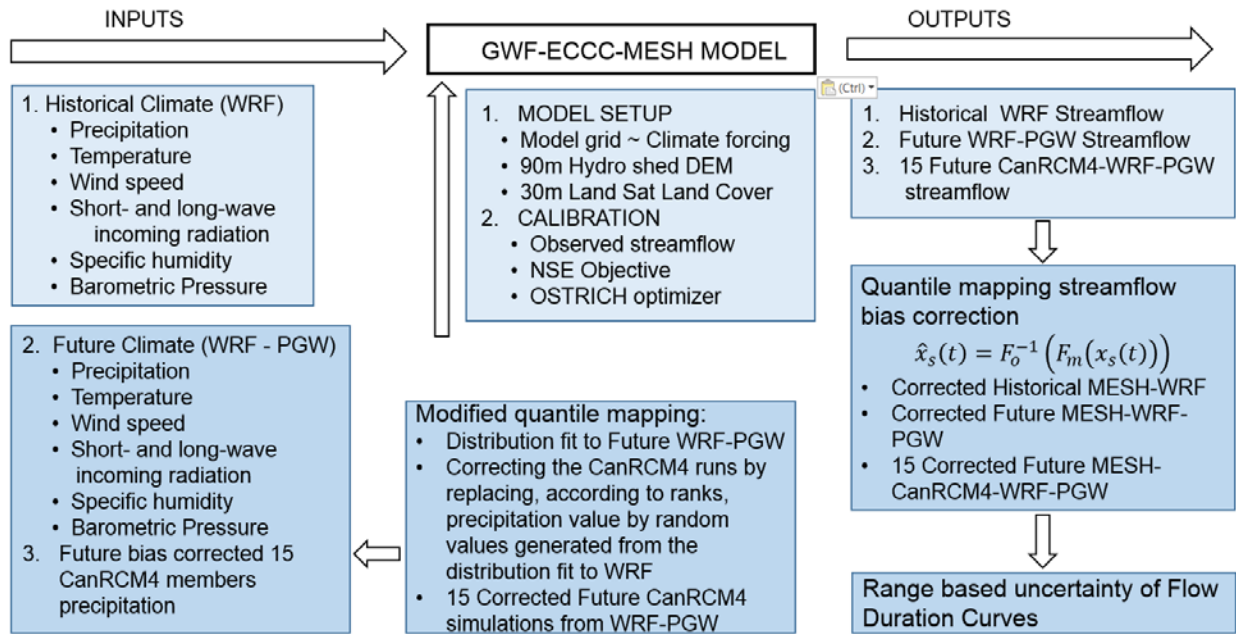


Figure 18. Flowchart conceptualising the methodology to calculate future flow duration curves (flood exceedance probabilities) with uncertainty from a high-resolution climate model and physically based hydrological model.

5.3 How to drive hydraulic models of flood plains using these outputs

Figure 19 illustrates how the proposed conceptual approach may be applied for hydraulic modelling and flood plain mapping. As per the procedure, the discharge data that will be used in the hydraulic modelling, flood mapping and mitigation activities are derived from the hydrological and climate modelling exercise described above. The simulated discharges for various flood frequency estimates, with their uncertainties ranges, were derived from an uncertain future climate (Figure 19). Routing the various frequencies, discharge and their uncertainties in pre-defined locations produced frequencies of water levels, and their uncertainties, at corresponding frequencies.

The results of the hydraulic modelling may then be combined with channel geometry and topographical information to generate water surface profiles and/or flood inundation maps. The maps, which can be produced for corresponding frequencies, with their uncertainty range, can be used to select or review flood mitigation measures and to map floodplains and areas of varying flood risk. Importantly, the changes in flood risk would be conveyed by such maps. Assessing the capacities of the existing hydraulic structures and their operational rules against the range of future flood estimates will help to identify and propose changes to structures and operational water management measures.

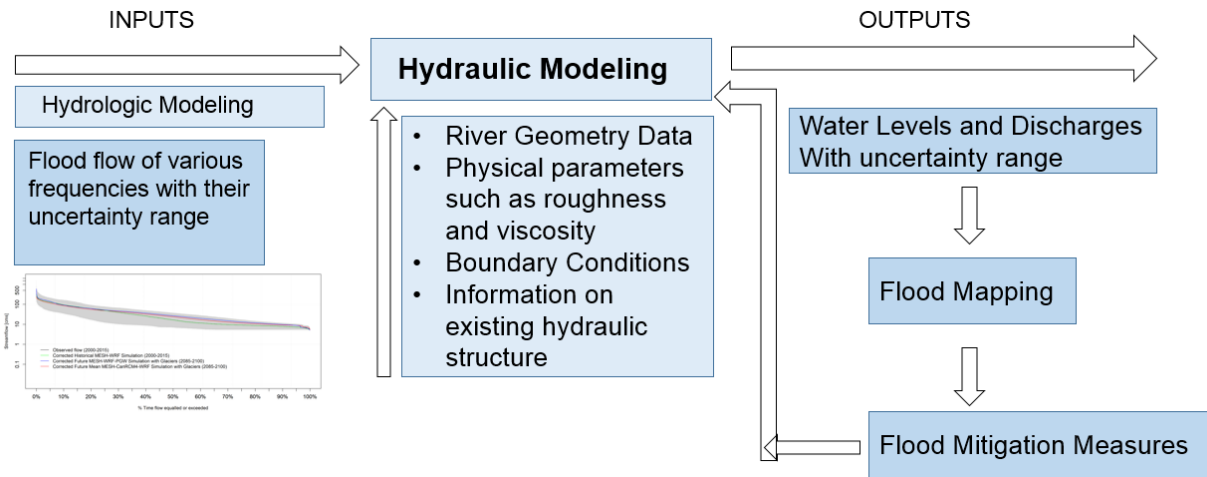


Figure 19 Proposed conceptual model of a national flood modelling and floodplain mapping methodology

6. Conclusions

In the Bow River Basin Study (BRBS) a coupled high resolution atmospheric regional model (WRF) and a hydrological model (MESH) provided reliable estimates of streamflow for the catchment. This coupled MESH-WRF was able to estimate streamflow quite well with minimal calibration of parameters in a mountainous watershed with complex topography. However, WRF has only a single run due to its high computational cost and so an assessment of uncertainty in streamflow estimation was not performed. This study advanced from the BRBS by assessing the uncertainty due to future precipitation by making use of an ensemble of 15 CanRCM4 regional climate simulations using varied boundary conditions. A novel correction scheme was developed to perturb the WRF Pseudo Global Warming run precipitation using the CanRCM4 simulations. In addition, frequency analyses were carried out for the City of Calgary to determine the changes projected in extreme precipitation.

The improved Mountain MESH model (including the effects of topography, slope and aspect) was set up, calibrated and run for the Bow and Elbow River Basins for several gridded meteorological datasets in the BRBS sister-study. The model setup incorporated simple reservoir operation rules that were developed by curve fitting techniques of the relationship between the quantiles of historical storage and releases as given in the main report. The model calibration was limited to a few routing and sub-surface parameters, with most parameters values selected from literature or previous studies. The very good performance of this model when compared to streamflow meant that it was chosen to be the hydrological model used in developing the flood estimation with uncertainty methodology in this report.

The effects of variability in CanRCM4 model outputs on simulated streamflow and flood frequencies were estimated for the Bow and Elbow river basins. Uncertainty in streamflow impacts due to inter-climate model variability of precipitation between the 15 CanRCM4s were simulated and found to be substantial and was greater than uncertainty from other climatic variables. The present study highlighted the usefulness of multi-CanRCM4 realizations in studies of hydrological impacts of climate change. While the WRF-driven hydrological simulations without uncertainty indicated a future decrease in the highest streamflows, the RCM-perturbed WRF-driven simulations showed that much higher streamflows are also possible under climate change. The flow duration curves developed from this study can be used to estimate flood frequency for floodplain mapping purposes if they are used as inputs to locally developed hydraulic models of the region of interest. The methodology shown here can be applied to river basins flowing into communities of interest across Canada. As a precondition for such applications a national gridded database of high resolution (4 km) WRF model downscaled climate model outputs that have been perturbed by multiple bias-corrected regional climate model realisations should be prepared as a forcing dataset for hydrological model applications. The MESH hydrological model evaluated here performed quite well when driven by high resolution WRF model outputs and should be examined for application to force local hydraulic models of flood inundation elsewhere in Canada. This is the basis for a coherent national approach to floodplain mapping that takes into account non-stationarity due to climate change.

7. References

- Asong ZE, Elshamy ME, Princz D, Wheeler HS, Pomeroy JW, Pietroniro A, Cannon A. (2020) High-resolution meteorological forcing data for hydrological modelling and climate change impact analysis in the Mackenzie River Basin. *Earth System Science Data*, 12(1).
- Cannon, A. J., Sobie, S. R., & Murdock, T. Q. (2015). Bias Correction of GCM Precipitation by Quantile Mapping: How Well Do Methods Preserve Changes in Quantiles and Extremes? *Journal of Climate*, 28(17), 6938–6959. <https://doi.org/10.1175/JCLI-D-14-00754.1>
- Côté, J., Gravel, S., Méthot, A., Patoine, A., Roch, M., & Staniforth, A. (1998). The Operational CMC–MRB Global Environmental Multiscale (GEM) Model. Part I: Design Considerations and Formulation. *Monthly Weather Review*, 126(6), 1373–1395. [https://doi.org/10.1175/1520-0493\(1998\)126<1373:TOCMGE>2.0.CO;2](https://doi.org/10.1175/1520-0493(1998)126<1373:TOCMGE>2.0.CO;2)
- Fang, X., & Pomeroy, J. W. (2007). Snowmelt runoff sensitivity analysis to drought on the Canadian prairies. *Hydrological Processes*, 21(19), 2594–2609. <https://doi.org/10.1002/hyp.6796>
- Grimaldi, S., Kao, S.-C., Castellarin, A., Papalexiou, S.-M., Viglione, A., Laio, F., et al. (2011). 2.18 - Statistical Hydrology. In P. Wilderer (Ed.), *Treatise on Water Science* (pp. 479–517). Oxford: Elsevier. <https://doi.org/10.1016/B978-0-444-53199-5.00046-4>
- Gudmundsson, L., Bremnes, J. B., Haugen, J. E., & Engen-Skaugen, T. (2012). Technical Note: Downscaling RCM precipitation to the station scale using statistical transformations – a comparison of methods. *Hydrology and Earth System Sciences*, 16(9), 3383–3390. <https://doi.org/10.5194/hess-16-3383-2012>
- IPCC. (2013). *Climate change 2013: the physical science basis Contribution of Working Group I to the Fifth Assessment Report of the Intergovernmental Panel on Climate Change* ed T F Stocker, D Qin, G K Plattner, M Tignor, S K Allen, J Boschung, A Nauels, Y Xia, V Bex and P M Midgley. Cambridge University Press.
- Li, Y., Li, Z., Zhang, Z., Chen, L., Kurkute, S., Scaff, L., & Pan, X. (2019). High-resolution regional climate modeling and projection over western Canada using a weather research forecasting model with a pseudo-global warming approach. *Hydrology and Earth System Sciences*, 23(11), 4635–4659. <https://doi.org/10.5194/hess-23-4635-2019>
- Rasmussen, R., Liu, C., Ikeda, K., Gochis, D., Yates, D., Chen, F., et al. (2011). High-Resolution Coupled Climate Runoff Simulations of Seasonal Snowfall over Colorado: A Process Study of Current and Warmer Climate. *Journal of Climate*, 24(12), 3015–3048. <https://doi.org/10.1175/2010JCLI3985.1>
- Rasmussen, R., Ikeda, K., Liu, C., Gochis, D., Clark, M., Dai, A., et al. (2014). Climate Change Impacts on the Water Balance of the Colorado Headwaters: High-Resolution Regional Climate Model Simulations. *Journal of Hydrometeorology*, 15(3), 1091–1116. <https://doi.org/10.1175/JHM-D-13-0118.1>

- von Salzen, K., McFarlane, N. A., & Lazare, M. (2005). The role of shallow convection in the water and energy cycles of the atmosphere. *Climate Dynamics*, *25*(7), 671–688. <https://doi.org/10.1007/s00382-005-0051-2>
- Salzen, K. von, Scinocca, J. F., McFarlane, N. A., Li, J., Cole, J. N. S., Plummer, D., et al. (2013). The Canadian Fourth Generation Atmospheric Global Climate Model (CanAM4). Part I: Representation of Physical Processes. *Atmosphere-Ocean*, *51*(1), 104–125. <https://doi.org/10.1080/07055900.2012.755610>
- Sanford, T., Frumhoff, P. C., Luers, A., & Gullede, J. (2014). The climate policy narrative for a dangerously warming world. *Nature Climate Change*, *4*(3), 164–166. <https://doi.org/10.1038/nclimate2148>
- Scinocca, J. F., Kharin, V. V., Jiao, Y., Qian, M. W., Lazare, M., Solheim, L., et al. (2016). Coordinated Global and Regional Climate Modeling. *Journal of Climate*, *29*(1), 17–35. <https://doi.org/10.1175/JCLI-D-15-0161.1>
- Tesemma, Z., Pomeroy, J. W., Rajulapati, C. R., & Shook, K. (2020). *Diagnosis of Historical and Future Flow Regimes of the Bow River at Calgary – Using a Dynamically Downscaled Climate Model and a Physically Based Land Surface Hydrological Model* (Centre for Hydrology No. xx). Saskatoon, Saskatchewan, Canada: Centre for Hydrology.
- Trenberth, K. (2011). Changes in precipitation with climate change. *Climate Research*, *47*(1), 123–138. <https://doi.org/10.3354/cr00953>
- Verseghy, D. (2012). *CLASS-the Canadian land surface scheme (version 3.6)* (No. Tech Rep 179). Environ Can Sci Technol Branch.
- Weedon, G. P., Gomes, S., Viterbo, P., Shuttleworth, W. J., Blyth, E., Österle, H., et al. (2011). Creation of the WATCH Forcing Data and Its Use to Assess Global and Regional Reference Crop Evaporation over Land during the Twentieth Century. *Journal of Hydrometeorology*, *12*(5), 823–848. <https://doi.org/10.1175/2011JHM1369.1>
- Whan, K., & Zwiers, F. (2016). Evaluation of extreme rainfall and temperature over North America in CanRCM4 and CRCM5. *Climate Dynamics*, *46*(11), 3821–3843. <https://doi.org/10.1007/s00382-015-2807-7>
- Whan, K., Zwiers, F., & Sillmann, J. (2016). The Influence of Atmospheric Blocking on Extreme Winter Minimum Temperatures in North America. *Journal of Climate*, *29*(12), 4361–4381. <https://doi.org/10.1175/JCLI-D-15-0493.1>
- Whitfield, P. H., & Pomeroy, J. W. (2016). Changes to flood peaks of a mountain river: implications for analysis of the 2013 flood in the Upper Bow River, Canada: Changes Affecting Flood Peaks of Upper Bow River. *Hydrological Processes*, *30*(25), 4657–4673. <https://doi.org/10.1002/hyp.10957>

Zhang, G. J., & McFarlane, N. A. (1995). Sensitivity of climate simulations to the parameterization of cumulus convection in the Canadian climate centre general circulation model. *Atmosphere-Ocean*, 33(3), 407-446. <https://doi.org/10.1080/07055900.1995.9649539>

Zhang, Z., Li, Y., Chen, F. et al. Evaluation of convection-permitting WRF CONUS simulation on the relationship between soil moisture and heatwaves *Clim Dyn* (2018). <https://doi.org/10.1007/s00382-018-4508-5>.